

Odd triplet pairing effects induced by interface spin-flip scatterings: critical temperature of superconductor/ferromagnet bilayers

Hyeonjin Doh^{1,*} and Han-Yong Choi^{1,2,†}

¹*Department of Physics, BK21 Physics Research Division,
Institute for Basic Science Research, Sung Kyun Kwan University, Suwon 440-746, Korea.*
²*Asia Pacific Center for Theoretical Physics, Pohang 790-784, Korea.*

The superconducting critical temperature T_C of a superconductor/ferromagnet (S/F) bilayer with spin-flip scatterings at the interface is calculated as a function of the ferromagnet thickness d_F in the dirty limit employing the Usadel equation. The appropriate boundary conditions from the spin-flip scatterings at the S/F interface are derived for the Usadel equation which includes the spin triplet pairing components as well as the spin singlet one. The spin-flip processes induce the spin triplet pairing components with s -wave in momentum and odd symmetry in frequency from the s -wave singlet order parameter Δ of the superconductor region. The induced triplet components alter the singlet order parameter in the superconductor through boundary conditions at the interface and, consequently, change the T_C of an S/F bilayer system. The calculated $T_C(d_F)$, like the case of no spin-flips, shows non-monotonic behavior which typically decreases as d_F is increased from 0 and shows a shallow minimum and then saturates slowly as d_F is further increased. It is well established that as the interface resistance (parameterized in terms of γ_b) is increased, the T_C is increased for a given d_F and the non-monotonic feature in $T_C(d_F)$ is strongly suppressed. As the spin flip scattering (parameterized in terms of γ_m) is increased, on the other hand, the T_C is also increased for a given d_F , but the non-monotonic feature in $T_C(d_F)$ is less suppressed or even enhanced, through the formation of the spin triplet components.

PACS numbers: PACS: 74.20.Rp, 74.45.+c, 74.62.-c, 74.62.Yb, 75.70.Cn

I. INTRODUCTION

The superconductivity and ferromagnetism are two competing orders: The former prefers a spin anti-parallel state and the latter a spin parallel state. They can coexist and exhibit interesting interplay effects only in a very narrow range of parameters. The effects of their competition and interplay, therefore, can be more conveniently studied when the interactions responsible for the two orders are confined to spatially separate regions of a system like a superconductor/ferromagnet (S/F) junction. When a superconductor is brought into a contact with a ferromagnet, the two competing orders influence each other in the vicinity of the interface on a spatial scale of the order of the coherence lengths. These phenomena of mutual influences are referred to as ‘‘proximity effects’’. The proximity effects of a superconductor/normal metal (S/N) junction show up as a penetration of the superconducting pairing amplitude into the normal metal region with an exponential decay^{1,2}. In an S/F junction, on the other hand, the superconducting pairing amplitude $\Psi(x)$ in the ferromagnet region does not simply decay exponentially but also oscillates. This oscillation shows up because the electrons forming Cooper pairs feel a distinct potential depending on their spin due to the exchange field in the ferromagnet, which leads to a finite momentum of a Cooper pair similar to the ‘‘Fulde-Ferrel-Larkin-Ovchinnikov state’’ (FFLO state) in bulk materials^{3,4}.

The same physics behind this pairing amplitude oscillation manifests itself in a number of different contexts: For instance, the non-monotonic dependence of T_C of S/F systems on the ferromagnet thickness d_F and the ‘‘ π -

state’’ of S/F/S junctions, among others. Here, the T_C is the superconducting critical temperature of an S/F junction where the current is parallel to the interface. Then, the T_C corresponds to the highest temperature at which the superconducting order parameter $\Delta(x)$ becomes non-vanishing at least at one point within the junction. The $\Delta(x)$ defined in Eq. (10) and $\Psi(x)$ are related as

$$\Delta(x) = \lambda\Psi(x), \quad (1)$$

where λ is the superconducting pairing interaction. The π -state refers to a case where two superconductors of a S/F/S junction separated by a ferromagnet of an appropriate thickness have the phase difference of π in a ground state without any external gauge field. That is, the order parameters of two superconducting regions have the opposite signs. The magnetic coherence length, which determines the oscillation length and the penetration depth of the pairing amplitude $\Psi(x)$ in the ferromagnet, the ferromagnet thickness d_F of minimum T_C in $T_C(d_F)$, the ferromagnet thickness of the π -junction, and so on, is given roughly by

$$\xi_F^{\text{ex}} = \begin{cases} \frac{\hbar v_F}{\pi E_{\text{ex}}} & \text{for clean limit,} \\ \sqrt{\frac{\hbar v_F \ell}{\pi E_{\text{ex}}}} & \text{for dirty limit,} \end{cases} \quad (2)$$

where E_{ex} is the exchange energy and ℓ is the mean free path. For a ferromagnet, E_{ex} is about thousands Kelvin, which gives a ξ_F^{ex} of a few nanometers. Studies of the oscillatory behavior of S/F junctions, therefore, require a fabrication technique of a nanometer scale control of the F thickness.

Due to the difficulties in the fabrication, serious studies of S/F junctions were initiated by theoretical works in the late 70's. Bulaevskii *et al.* considered magnetic impurities in Josephson junction⁵. Buzdin *et al.* predicted the critical current⁶ and T_C oscillation⁷ as a function of d_F , and studied the effects of ferromagnet layer in Josephson junction⁸. Following these theoretical works, many experimental efforts have been made to test the pairing amplitude oscillation in the ferromagnet. One of them is to measure the T_C vs. d_F of S/F bilayers. The measured T_C showed a non-monotonic dependence on d_F ⁹, although there were some contradictory reports¹⁰. Another line of research is to verify the π -state. Quite a few experiments reported the π -state: tunneling spectroscopy¹¹, temperature dependence¹², and thickness dependence of the critical current¹³, and even phase sensitive measurements¹⁴. Through all the above experiments, the pairing amplitude oscillation in the superconductor-ferromagnet hetero structures is now well established.

The advancement of the experimental technique of the S/F systems, on the other hand, demanded more detailed theoretical analysis of the systems to include those effects hitherto not considered such as the inhomogeneity of the magnetization. For example, there were some measurements that reported much longer penetration lengths in S/F junctions^{15,16}. The T_C difference between the parallel and anti-parallel magnetizations of the two ferromagnets sandwiching the superconductor in F/S/F junctions is smaller by the factor of 10^2 than the theory predicts¹⁷. For filling the gap between the theories and experiments, the spin-orbit scattering in the ferromagnet¹⁸, or the triplet components¹⁹⁻²⁴ began to be considered by several groups. It should be pointed out that there is *no* pairing interaction in the triplet channel in the S or F region because conventional *s*-wave superconductors were considered for S/F bilayer junctions.

The triplet pairing components are induced in a hybrid junction of S and F when a single quantization axis for spin can *not* be defined for the whole junction. Such situations arise and the triplet pairings were studied for (a) the non-collinear alignment of the magnetic moments of two F's in a F/S/F structure²²⁻²⁴ [Fig. 1 (a)], (b) a rotation of the magnetization direction within a finite thickness in a F region of S/F bilayers¹⁹ [Fig. 1 (b)], (c) spin-orbit scattering near the interface between non-magnetic and magnetic materials in S/F structures²⁰, and (d) spin mixing near the interfaces of S/F/S structure where F is a half-metal²¹. The works of (a)-(b) considered the dirty limit cases. In the dirty limit, the non-*s* wave components are strongly suppressed, and the so called "odd" frequency triplet superconductivity is more robust than the *p*-wave triplet superconductivity. The odd triplet pairing has even symmetry in spin and momentum spaces but odd symmetry in frequency, and was first proposed by Berezinskii²⁵ in 1974 in the context of ³He superfluidity. The odd frequency triplet pairings, interestingly, can be realized in hybrid junctions of S and F as discussed in (a)-(b) which employed the Usadel equation in the dirty

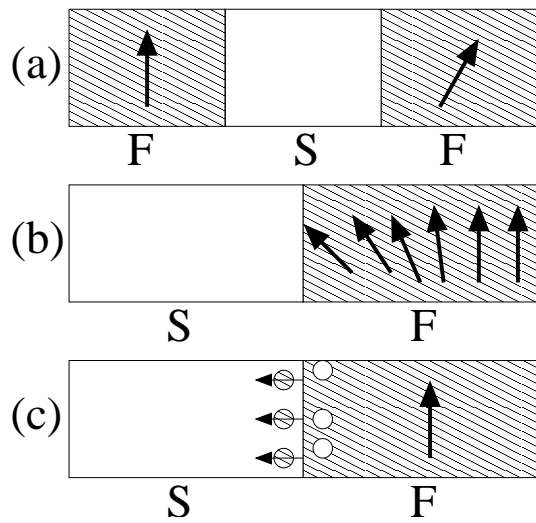


FIG. 1: Some schematic pictures of cases which can induce the triplet pairing components. (a) non-collinear magnetizations of two ferromagnets separated by a superconducting layer, (b) rotation of magnetization in a ferromagnet layer, and (c) spin-flip scattering at the interface of the magnetic and the non-magnetic layers due to mixing of two materials or spin-orbit scattering.

limit²⁶. The work (c)-(d) considered the *p*-wave pairing in the clean limit.

In this paper, we considered an S/F bilayer as in (b) and (c), and studied the effects of the induced triplet pairing components in S/F bilayers by employing the Usadel equation. The difference is that we consider the spin flip scatterings at the interface. Technically, this calls for new boundary conditions at the interface of an S/F junction. We derived such boundary conditions accommodating the spin-flip scatterings at the interface. The work of (b) simplified and bypassed the problem of the new boundary conditions by considering an artificial rotation of the magnetization of a fixed amplitude in the F region. On the other hand, we consider an intrinsic magnetic inhomogeneity at the interface of S/F junctions as depicted in Fig. 1 (c). The Usadel equation is appropriate in the dirty limit and is widely employed for analyzing various S/N, S/F, and S/N/F systems since various junctions of S, N and F films belong to the dirty limit. Here, we calculate the critical temperature T_C as a function of the ferromagnet thickness d_F of S/F bilayers including the triplet pairing components in addition to the singlet one.

This paper is organized as follows. In Sec. II, we will introduce the notations and write down the Usadel equation and boundary conditions that need to be solved. For the boundary conditions of Usadel equation with spin-flip scatterings, the boundary conditions of the Eilenberger equation is first derived in the Appendix A and, in Appendix B and C, the detailed derivation of the boundary conditions for Usadel equation is collected. This will render the paper more easily accessible to the less technically

inclined. Then, the Usadel equation with the appropriate boundary conditions is mapped onto an eigenvalue problem [See Eq. (24) below.] whose detailed derivation is given in Appendix D. Actual calculations of T_C constitute setting up the matrix K_{ij} of Eq. (24) and finding its smallest eigenvalue self-consistently. The self-consistency is achieved via iterations. In Sec. III, the results of numerical T_C calculations of S/F bilayers with the spin-flip scattering induced triplet components will be presented. Overall, the T_C of S/F bilayers with the spin-flip scatterings, like the more familiar case of no spin-flips, typically decreases initially as d_F is increased from 0, then shows a minimum at a finite d_F , then increases slowly and saturates to $T_C^* = T_C(d_F \rightarrow \infty)$ as d_F is further increased. As the spin flip scatterings are increased, compared with the corresponding no spin flip case, (a) the T_C is increased with decreasing non-monotonic behavior, but (b) the relative non-monotonic feature in $T_C(d_F)$ with respect to T_C^* is enhanced (the increase of T_C^* is faster than the minimum T_C), through the formation of spin triplet components. Finally, we have summary and some concluding remarks in Sec. IV.

II. FORMULATION OF S/F BILAYER

In this section, we will present the Usadel equation with the induced odd-frequency s -wave triplet pairing components in addition to the dominant singlet pairing order parameter, boundary condition at the S/F interface, and calculation of T_C by mapping onto an eigenvalue problem. The detailed derivations of the boundary conditions and mapping of T_C to the eigensystem are collected in the Appendix B, and D, respectively. We consider the dirty limit case which almost all experiments belong to.

The Usadel equation which considers both the singlet and triplet pairing components can be written using the anomalous function in spin space as follows:

$$\xi^2 \pi T_C \frac{\partial^2}{\partial x^2} \hat{F}(x, i\omega) = |\omega| \hat{F}(x, i\omega) - \hat{\Delta}(x) \quad (3)$$

$$-i \operatorname{sgn}(\omega) \left(\hat{H}_{\text{ex}} \hat{F}(x, i\omega) - \hat{F}(x, i\omega) \hat{H}_{\text{ex}}^* \right),$$

where \hat{F} is the Usadel function from anomalous Green's function of 2×2 matrix in spin space and $\hat{\Delta}$ is the singlet pairing order parameter.

$$\hat{F} = \begin{bmatrix} F_{\uparrow\uparrow} & F_{\uparrow\downarrow} \\ F_{\downarrow\uparrow} & F_{\downarrow\downarrow} \end{bmatrix}, \quad \hat{\Delta} = \begin{bmatrix} 0 & \Delta \\ -\Delta & 0 \end{bmatrix} \quad (4)$$

\hat{H}_{ex} is also 2×2 matrix which denotes the exchange field in the ferromagnet.

$$\hat{H} = H_{\text{ex}}^x \sigma_x + H_{\text{ex}}^y \sigma_y + H_{\text{ex}}^z \sigma_z \quad (5)$$

where σ_i 's are the Pauli matrices. To show the coupling between the singlet and triplet pairing state clearly, the

following vector form of the Usadel equation can be convenient in numerical calculations.

$$\xi^2 \pi T_C \frac{\partial^2}{\partial x^2} \mathbf{F}(x, i\omega) = |\omega| \mathbf{F}(x, i\omega) - \mathbf{\Delta}(x) - i \operatorname{sgn}(\omega) \mathbf{H}_{\text{ex}} \cdot \mathbf{F}(x, i\omega), \quad (6)$$

where $\omega = 2\pi T(n + 1/2)$ is the Matsubara frequency, $D = v_F^2 \tau / 3$ is the diffusion constant, and

$$\xi = \sqrt{D / 2\pi T_C} \quad (7)$$

is the coherence length in dirty limit. The \mathbf{F} and $\mathbf{\Delta}$ are four component vectors and \mathbf{H}_{ex} is a 4×4 exchange field tensor given, respectively, by

$$\mathbf{F}(x, i\omega) = \begin{bmatrix} F_s(x, i\omega) \\ F_{tx}(x, i\omega) \\ F_{tz}(x, i\omega) \\ F_{t0}(x, i\omega) \end{bmatrix}, \quad \mathbf{\Delta}(x) = \begin{bmatrix} \Delta(x) \\ 0 \\ 0 \\ 0 \end{bmatrix},$$

$$\mathbf{H}_{\text{ex}} = \begin{bmatrix} 0 & -H_{\text{ex}}^z & -H_{\text{ex}}^x & -iH_{\text{ex}}^y \\ -H_{\text{ex}}^z & 0 & 0 & 0 \\ -H_{\text{ex}}^x & 0 & 0 & 0 \\ iH_{\text{ex}}^y & 0 & 0 & 0 \end{bmatrix}. \quad (8)$$

$\Delta(x)$ is the singlet s -wave pairing order parameter and a function of x which represents the coordinate perpendicular to the interface between S and F. The F_α 's are transformations of the $F_{\sigma\sigma'}$ by expanding \hat{F} on the basis of the Pauli matrices as shown in Eq. (B14) in Appendix B. The transformations are given as:

$$F_s = \frac{1}{2}(F_{\uparrow\downarrow} - F_{\downarrow\uparrow}), \quad F_{tx} = \frac{1}{2}(F_{\uparrow\downarrow} + F_{\downarrow\uparrow}),$$

$$F_{tz} = \frac{1}{2}(F_{\uparrow\uparrow} - F_{\downarrow\downarrow}), \quad F_{t0} = \frac{1}{2}(F_{\uparrow\uparrow} + F_{\downarrow\downarrow}). \quad (9)$$

The F_s is the singlet pairing component and the others are the triplet pairing components. The self-consistency relation is given by

$$\Delta(x) = \lambda \pi T_C g(\epsilon_F) \sum_{\omega_n} F_s(x, i\omega_n), \quad (10)$$

where λ is the superconducting pairing interaction and $g(\epsilon_F)$ is the density of states per spin at the Fermi level. Since we assume that λ is zero at ferromagnet, we should note that the superconducting order Δ is also zero at ferromagnet and that only the pairing amplitude Φ can penetrate into.

The Usadel equation of Eq. (3) or (6) must be supplemented by a set of appropriate boundary conditions. The system we consider is an S/F junction where the interface between S and F has the potential (without spin-flip) and spin-flip scatterings due to magnetic inhomogeneity as shown in Fig. 2. Therefore, the interface potential is represented by δ functions with the spin dependency as

$$U(x) = (V_0 \sigma_0 + V_x \sigma_x + V_y \sigma_y + V_z \sigma_z) \delta(x). \quad (11)$$

For simplicity, we can set V_0 and V_x to be the only non-zero parameters among the spin dependent δ -function, when the magnetization of ferromagnetic layer is in z -direction. The spin-flip scatterings were modeled in terms of the δ -function-like magnetization at the interface. In real situations, this will be local inhomogeneities of the magnetization within a very short range near the interface. Within the Usadel formulation, the boundary conditions using the similar notation with Eq. (6) can be written as

$$\mathbf{F}^S - \mathbf{F}^F = [\hat{\gamma}_b - i \operatorname{sgn}(\omega)\hat{\gamma}_m] \xi_F \frac{\partial}{\partial x} \mathbf{F}^F, \quad (12)$$

$$\xi_S \frac{\partial}{\partial x} \mathbf{F}^S - \gamma \xi_F \frac{\partial}{\partial x} \mathbf{F}^F = 0, \quad (13)$$

where the dimensionless parameters are defined by

$$\gamma = \frac{\rho_S \xi_S}{\rho_F \xi_F}, \quad \hat{\gamma}_b = \begin{bmatrix} \gamma_b + \gamma_1 & 0 & 0 & 0 \\ 0 & \gamma_b - \gamma_1 & 0 & \gamma_2 \\ 0 & 0 & \gamma_b + \gamma_1 & 0 \\ 0 & \gamma_2 & 0 & \gamma_b - \gamma_1 \end{bmatrix},$$

$$\hat{\gamma}_m = \begin{bmatrix} 0 & 0 & \gamma_m & 0 \\ 0 & 0 & 0 & 0 \\ \gamma_m & 0 & 0 & 0 \\ 0 & 0 & 0 & 0 \end{bmatrix}. \quad (14)$$

The γ is the ratio of S and F bulk properties, and γ_b represents the contact quality which is expressed as $\frac{\mathcal{R}\mathcal{A}}{\rho_F \xi_F}$ without spin-flip scatterings. \mathcal{A} and \mathcal{R} are the interface area and resistance, respectively. γ_m is the spin-flip strengths between S and F which is proportional to V_x in (11). γ_1 and γ_2 comes from the higher order term of V_x and V_0 which can be ignored when the scattering strength is weak. See Appendix B for details.

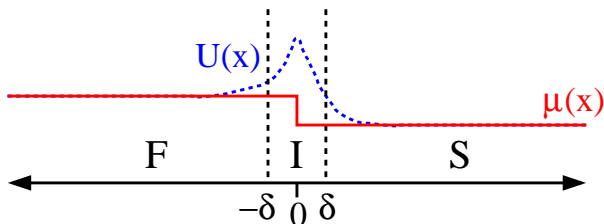


FIG. 2: The hypothetical layer (I) with an infinitesimal thickness 2δ between superconductor (S) and ferromagnet (F) which are described as a spin-dependent potential $U(x)$ which will give a interface resistance and a spin-flip scattering. $\mu(x)$ stands for a local chemical potential.

The Usadel equation of Eq. (6) with the boundary conditions of Eqs. (12) and (13) was mapped onto an eigenvalue problem and solved numerically to determine the T_C . The T_C defined here can be determined experimentally by measuring the resistance with the current parallel to the interface. For simplicity, we take the magnetization at the interface along the x -axis and that of ferromagnet along the z -axis.

We follow Fominov *et al.*^{27,28} to get the numerical solution of the Usadel equation. We first separate the anomalous Green's function $F_\alpha(x, i\omega)$ into the even and odd symmetry parts in the frequency space

$$F_\alpha^{(\pm)}(x, i\omega) = F_\alpha(x, i\omega) \pm F_\alpha(x, -i\omega), \quad (15)$$

where $\alpha = s, tx, tz,$ and $t0$. Since all the anomalous Usadel functions are s -wave pairing, we choose the even symmetry in frequency for the singlet component, and the odd symmetry for the triplet components. Thus we define a 4-component vector \mathcal{F} as

$$\mathcal{F}(x, i\omega) \equiv \begin{bmatrix} F_s^{(+)}(x, i\omega) \\ F_{tx}^{(-)}(x, i\omega) \\ F_{tz}^{(-)}(x, i\omega) \\ F_{t0}^{(-)}(x, i\omega) \end{bmatrix}. \quad (16)$$

Here, the triplet components, F_{tx} , F_{tz} and F_{t0} , are odd in the frequency and even in the momentum space as we mentioned in Sec. I. This special type of triplet pairing is the odd triplet pairing proposed by Berezinskii²⁵. It will be much more robust than a p -wave triplet pairing to disorders due to the momentum independent gap feature.

As shown in Fig. 3, for an S/F bilayer, we took the superconductor region in $0 < x < d_S$, the ferromagnet in $-d_F < x < 0$, and the spin-flip scatterings at the interface of $x = 0$. In the S region, there is no exchange field and only pairing order parameter $\Delta(x)$ exists. Therefore, the Usadel equation of (6) can be written for the S region as

$$\pi T_C \xi_S^2 \frac{\partial^2}{\partial x^2} \mathcal{F}^S(x, i\omega) = |\omega| \mathcal{F}^S(x, i\omega) - 2\Delta(x), \quad (17)$$

for $0 < x < d_S$. For the F region, on the other hand, there is no pairing interaction and only the exchange field term appears. The Usadel equation is then written as

$$\pi T_C \xi_F^2 \frac{\partial^2}{\partial x^2} \mathcal{F}^F(x, i\omega) = (|\omega| - i\hat{\mathbf{H}}_{\text{ex}}) \mathcal{F}^F(x, i\omega), \quad (18)$$

for $-d_F < x < 0$. The coherence length ξ_F in the F region is given by Eq. (7) as

$$\xi_F = \sqrt{\frac{D_F}{2\pi T_C}}, \quad (19)$$

where D_F is the diffusion constant of F and T_C is the superconducting transition temperature of the S/F junction. The ξ_F should be distinguished from the ξ_F^{ex} of Eq. (2). ξ_F^{ex} corresponds to the actual penetration depth of singlet pairing amplitude in F, but ξ_F is the pure penetration depth without considering the exchange field as in normal metal. Later, this ξ_F will turn out to be a penetration depth of triplet components, F_{tz} and F_{t0} , which is unaffected by the exchange energy. The boundary conditions of Eqs. (12) and (13) can be written in terms of

$\mathcal{F}(x, i\omega)$ of Eq. (16) as follows:

$$\frac{\partial}{\partial x} \mathcal{F}^S(d_S) = 0, \quad \frac{\partial}{\partial x} \mathcal{F}^F(-d_F) = 0, \quad (20)$$

$$\mathcal{F}^S(0) - \mathcal{F}^F(0) = \hat{\gamma}_b \xi_F \frac{\partial}{\partial x} \mathcal{F}^F(0), \quad (21)$$

$$\xi_S \frac{\partial}{\partial x} \mathcal{F}^S(0) - \gamma \xi_F \frac{\partial}{\partial x} \mathcal{F}^F(0) = 0, \quad (22)$$

where

$$\hat{\gamma}_b = \begin{bmatrix} \gamma_b & 0 & -i\gamma_m & 0 \\ 0 & \gamma_b & 0 & 0 \\ -i\gamma_m & 0 & \gamma_b & 0 \\ 0 & 0 & 0 & \gamma_b \end{bmatrix}. \quad (23)$$

Here, γ_1 and γ_2 of Eq. (14) are ignored for the weak scattering rate at the interface.

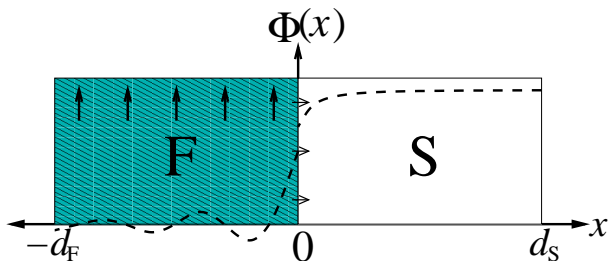


FIG. 3: A schematic plot of the pairing amplitude $\Phi(x)$ of Eq. (10) with the dotted line for an S/F bilayer. The magnetization in the ferromagnet region is taken in the z -direction and the magnetization at the S and F interface is in the x -direction.

As detailed in Appendix D, Eqs. (17), (18), (20), (21), and (22) can be solved for the T_C of a S/F bilayer, and the T_C equation with respect to the bulk transition temperature T_{C0} may be cast into the form

$$\Delta_i \ln \left(\frac{T_{C0}}{T_C} \right) = \sum_j^N K_{ij} \Delta_j, \quad (24)$$

where the order parameter Δ and kernel K are defined on a discrete grid as

$$\begin{aligned} \Delta_i &\equiv \Delta \left(\frac{d_S}{N} i \right), \\ K_{ij} &\equiv 2\pi T_C \sum_{\omega_n > 0} \left[\frac{\delta_{ij}}{|\omega_n|} - G_{ij}(i\omega_n) \right], \\ G_{ij}(i\omega_n) &\equiv \frac{d_S}{N} G \left(\frac{d_S}{N} i, \frac{d_S}{N} j, i\omega_n \right). \end{aligned} \quad (25)$$

Here, N is the number of the discrete grids in the integral domain between 0 and d_S . The T_C is determined by the smallest eigenvalue of the matrix K given by (25), which gives the largest T_C . However, the kernel K_{ij} is T_C dependent through the Matsubara frequencies $\omega_n = 2\pi T_C(n + 1/2)$. Therefore, we solve the Eq. (24) iteratively until it gives a self-consistent solution for T_C .

III. NUMERICAL RESULTS

The interface parameter of the boundary condition, $\hat{\gamma}_b$ in (21), contains diagonal and off-diagonal elements as given in (23). The diagonal element, γ_b , corresponds to the interface resistance and the off-diagonal element, γ_m , to the scattering between singlet and triplet pairing components. The relation between the parameters γ_b , γ_m and the more microscopic processes like the potentials V_0 , V_x is complicated and depends on detailed mechanism. In the present work, therefore, we take the γ_b and γ_m in (23) as independent parameters characterizing the S/F interface without explicit references to more microscopic processes. For the present microscopic consideration in terms of V_0 and V_x , the connection between the interface parameters and the microscopic potentials can be found in Appendix B.

The Usadel equations in Eqs. (17) and (18) with the boundary condition in Eqs. (20), (21), and (22), can be expressed by the seven dimensionless parameters, d_S/ξ_S , d_F/ξ_F , T_C/T_{C0} , H_{ex}/T_{C0} , γ , γ_b , and γ_m . All the calculations for T_C/T_{C0} are done and shown in the figures with respect to the other six independent parameters. The numerical results were calculated based on the parameters in Ref. 28, which are $T_{C0} = 7.0$ K, $\xi_S = 8.9$ nm, $\xi_F = 7.6$ nm, $\rho_S = 7.5 \mu\Omega\text{cm}$, $\rho_F = 60.0 \mu\Omega\text{cm}$, and $d_S = 11$ nm.

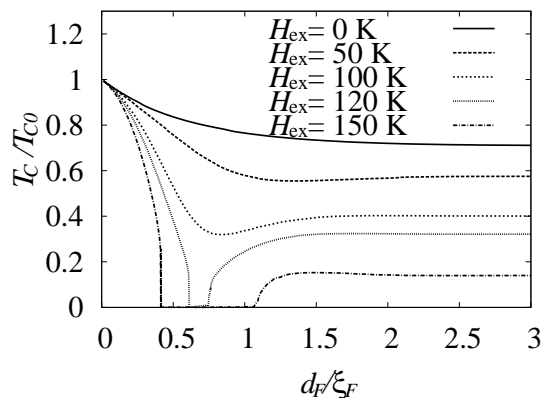


FIG. 4: T_C/T_{C0} vs. d_F/ξ_F for the various H_{ex} without interface resistance and spin-flip scattering at the interface, i.e. $\gamma_b = 0.0$ and $\gamma_m = 0.0$.

First, we show the typical behavior of $T_C(d_F)$ in S/F bilayer in Fig. 4 as well as $T_C(d_N)$ in S/N bilayer (solid line) which is S/F bilayer with zero exchange field, $H_{ex} = 0.0$. For S/N bilayer, T_C decreases monotonically as the thickness of normal metal layer increases. When the exchange field is turned on, the T_C 's, the dotted curves in Fig. 4, show typical behaviors of $T_C(d_F)$ for S/F bilayers. As d_F is increased from 0, T_C decreases fast initially and shows a minimum, and then increases slightly and saturates as d_F is further increased. This non-monotonic dependence of T_C on d_F is due to the oscillation of the pairing amplitude in ferromagnet, known

as FFLO state. The thickness of minimum T_C in $T_C(d_F)$ is almost corresponding to the dirty limit value of ξ_F^{ex} in Eq. (2). For the same reason, the minimum T_C can be also denoted as the transition from 0-state to π -state of pairing amplitude in F. As shown in Eq. (2), the position of minimum T_C is shifted to left as H_{ex} increases. For a strong enough exchange energy, T_C is strongly suppressed and goes to zero as d_F increases.²⁸ For a properly strong exchange field, moreover, the reentrant behavior of superconductivity occurs as the cases of $H_{\text{ex}} = 120$ K and 150 K shown in Fig. 4.

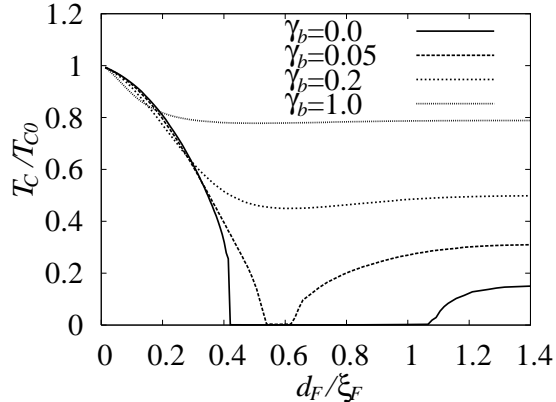


FIG. 5: T_C/T_{C0} vs. d_F/ξ_F for the various γ_b without spin-flip scattering at the interface, i.e. $\gamma_m = 0.0$.

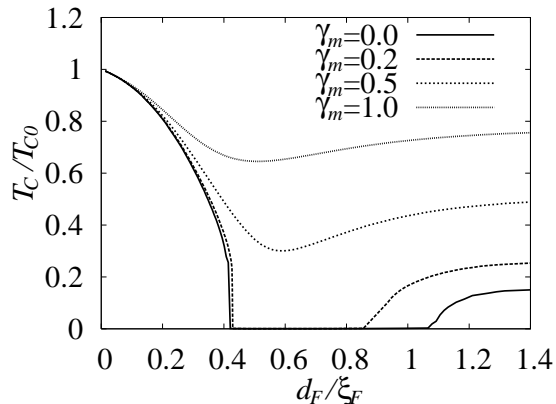


FIG. 6: T_C/T_{C0} vs. d_F/ξ_F for the various γ_m with spin-flip scattering at the interface with $\gamma_b = 0.0$.

Fig. 5 shows the effects of interface resistance on the F thickness, d_F , dependence of the superconducting critical temperature T_C of S/F bilayers. All the parameters except for γ_b are same as used in Fig. 4 and the exchange field is fixed to $H_{\text{ex}} = 150$ K. As the interface resistance parameter γ_b is increased, the $T_C(d_F)$ is increased and the non-monotonic feature becomes weakened. The T_C is increased because a large γ_b decouples S from F and, therefore, S is not influenced by F. Fig. 5 shows that the non-monotonic feature is almost washed out for $\gamma_b \gtrsim 0.2$.

In Fig. 6, $T_C(d_F)$ is calculated for various γ_m , the interface spin flip parameter, with the other parameters same as in Fig. 5. A non-zero γ_m induces the triplet pairing components and couples them with the singlet component. As can be seen from the figure, T_C is enhanced by γ_m as well. Recall that T_C is determined by the singlet pairing order parameter $\Delta(x)$ in the S region, and there is no pairing interaction in the triplet channel for the S/F system we consider here. The triplet components come into existence only through γ_m , and an increase of γ_m means an increase of the triplet pairing components. The T_C is enhanced because the singlet pairing order parameter $\Delta(x)$ in the S region is enhanced when it is coupled to the triplet components in addition to the singlet pairing component. The exchange field of F region does not act as a pair breaker for the triplet components unlike for the singlet one. The detail effects of the γ_m is somewhat different from γ_b . When we compare two cases of $\gamma_b = 0.2$ in Fig. 5 and $\gamma_m = 0.5$ in Fig. 6, both have almost same saturated $T_C^* \equiv \lim_{d_F \rightarrow \infty} T_C(d_F)$, but the non-monotonic structure is much stronger in the later case than the former one. While the γ_m is similar to γ_b in the sense of the increase of T_C and the suppression of a minimum T_C at a particular d_F , they are different in that the non-monotonic structure is less suppressed by γ_m than by γ_b . This can be more clearly when the

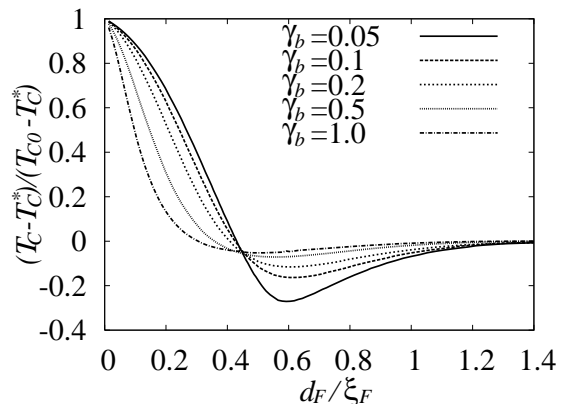


FIG. 7: $(T_C - T_C^*)/(T_{C0} - T_C^*)$ vs. d_F/ξ_F for several values of the interface resistance parameter γ_b with the interface spin-flip scattering parameter $\gamma_m = 0.2$. As the γ_b is increased, the non-monotonic feature is successively weakened. The T_C increases as γ_b is increased but appears the other way because it is normalized as Eq. (26).

$T_C(d_F)$ is normalized in the following way:

$$(T_C - T_C^*)/(T_{C0} - T_C^*). \quad (26)$$

Fig. 7 and Fig. 8 show how the non-monotonic feature changes as γ_b and γ_m , respectively, are increased from $\gamma_b = 0.05$ and $\gamma_m = 0.2$. Both figures were calculated with the same parameter set as in Fig. 5 and Fig. 6 except for the γ_b and γ_m . The results for $\gamma_b = 0.05$ and $\gamma_m = 0.2$ are common for both figures and denoted

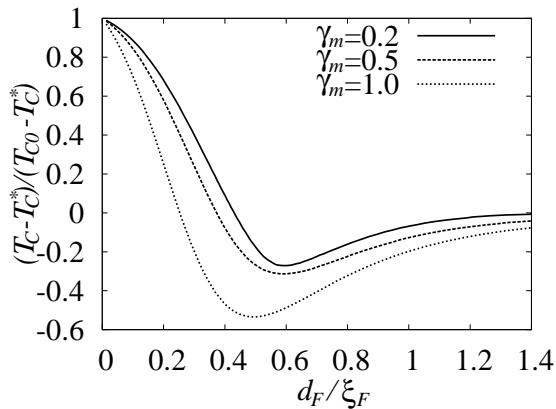


FIG. 8: $(T_C - T_C^*) / (T_{C0} - T_C^*)$ vs. d_F / ξ_F for various γ_m with $\gamma_b = 0.05$. Notice that an increase of γ_m enhances the non-monotonic feature.

as the solid lines. In Fig. 7, the minimum values of the normalized T_C increase, or the non-monotonic feature is weakened, as γ_b increases, while the minimum values decrease due to γ_m in Fig. 8. This means that the enhancement of minimum T_C is less strong than that of T_C^* . The reason is that the magnitude of the induced triplet components depend on the thickness of the ferromagnet of a S/F bilayer. The length scale over which the triplet components develop is given by $\xi_F \sim 1/k_F^0$ as in (D6) which is longer than that of singlet component in ferromagnet given by ξ_F^{ex} of Eq. (2). Therefore, the $T_C(d_F)$ with non-zero γ_m , compared with $T_C(d_F)$ with $\gamma_m = 0$, is increased more for $d_F > \xi_F$ than for $d_F < \xi_F$.

Another way of seeing why the magnitude of the induced triplet components depend on the ferromagnet thickness is from the boundary conditions of Eqs. (20) and (21). The boundary condition of (21) means that the magnitude of the triplet components are proportional to the derivative of the singlet component at the interface. Since the derivative of the pairing components at $x = -d_F$ is equal to 0 from (20), the derivative at $x = 0$ will be close to 0 when d_F approaches 0. This observation means that the magnitude of the triplet components also go to 0 as d_F goes to 0, and the enhancement of T_C due to the induced triplet components is not as strong for small d_F as for large d_F . Since the d_F at which the $T_C(d_F)$ is the minimum is about ξ_F^{ex} which is smaller than ξ_F , the enhancement of T_C for $d_F > \xi_F$ gives relative increase of the non-monotonic structure. This enhancement of the normalized non-monotonic feature is quite distinguishable from the effects of interface resistance and spin-orbit scattering in bulk ferromagnet¹⁸, which give the suppression of the non-monotonic structure.

IV. CONCLUSION

In this paper, we considered the effects of the odd-frequency s -wave triplet pairing components on the tran-

sition temperature vs. the ferromagnet thickness of S/F bilayers. The triplet pairing components are induced by the spin-flip scatterings at the interface. The interface spin-flips physically occur because the magnetic and non-magnetic atoms diffuse around the interface between the magnetic and non-magnetic layers, because the direction of magnetization is changed locally near the interface due to the boundary effects, or because the spin-orbit scattering at the interface induced by the polarization due to the difference of the work-function of two adjacent material.²⁰ The spin-flip scatterings at the interface were simply modeled in terms of a spin-dependent δ -function which includes potential scattering and spin-flip scattering. The appropriate boundary conditions describing the spin-flip scatterings at the interface between S and F were derived in the context of the Usadel equation and Eilenberger equation. Through the boundary condition, the singlet and triplet pairing components are coupled each other. The Usadel equation with the derived boundary conditions for S/F bilayers was then mapped onto an eigenvalue problem. It was solved self-consistently via iterations to obtain the superconducting transition temperature T_C of S/F bilayers.

Compared with no spin-flip cases, T_C is enhanced by inducing the triplet pairing components via spin-flip scatterings at the interface. In detail, this enhancement is distinguishable from the enhancement of other effects, for example, the interface resistance and the spin-orbit scattering in bulk ferromagnet. All these effects mostly suppress non-monotonic dependence in T_C vs. d_F , but the enhancement of T_C due to the spin flip scatterings is accompanied by an enhancement of the relative depth of minimum T_C which is scaled by the difference between T_{C0} and the saturated value, T_C^* . This enhancement of the relative non-monotonic structure in $T_C(d_F)$ is related to the coherence length ξ_F which is the decay length of triplet pairing state in ferromagnet. But the triplet pairing components affect $T_C(d_F)$, and can be distinguished from other effects by quantitative analysis of $T_C(d_F)$ measurements or tunneling experiments.

We are currently extending the present analysis to the superconductor/normal metal/ferromagnet (S/N/F) trilayer systems. The results will be reported separately.

Acknowledgments

We would like to thank Kookrin Char and Yong-Joo Doh for having brought this problem to our attention and for many helpful comments and discussions. This work was supported by the Korea Science & Engineering Foundation (KOSEF) through grant No. R01-1999-000-00031-0, and by the Ministry of Education through BK21 SNU-SKKU Physics program.

APPENDIX A: BOUNDARY CONDITIONS FOR EILENBERGER EQUATION

Since the quasi-classical equations such as Usadel equation and Eilenberger equation describe variation of physical quantity over longer length scale than interatomic length scale, they are invalid in dealing with the effects of interface directly. To include the spin-flip effects at the interface in the quasi-classical equations, we will impose such effects on the boundary condition. Since the Usadel equation is originated from the Eilenberger equation and the Eilenberger equation is again from Gor'kov's equation, the derivation of the boundary condition consists of two steps. First, we will derive the boundary condition for Eilenberger equation which is the quasi-classical

approximation of Gor'kov's equation. From Eilenberger equation, we will derive the boundary condition for Usadel equation which is the dirty limit of Eilenberger equation. The boundary condition for the Eilenberger equation without any spin-flip scattering at the interface is originally derived by Zaitsev²⁹. Therefore, we will follow his procedures and then include the spin degrees of freedom and spin-dependent interface potential for the spin-flip scattering at the interface. For the insufficient part in this derivation, readers refer to Ref. 29.

First, we write down the Gor'kov's equation, which describes the system of two adjacent region separated by intermediate region with thickness 2δ , as shown in Fig. 2.

$$\delta(\mathbf{r} - \mathbf{r}')\delta(\tau - \tau')\check{\mathbf{I}} = \left(-\rho_z \frac{\partial}{\partial \tau} + \frac{1}{2m} \frac{\partial^2}{\partial \mathbf{r}^2} + \check{\Delta} - U(\mathbf{r}) - \check{\Sigma} + \mu(\mathbf{r}) \right) \check{\mathbf{G}}(\mathbf{r}, \mathbf{r}'; \tau, \tau'), \quad (\text{A1})$$

where \check{G} is 4×4 Green's function in Nambu-Gor'kov space. $\mu(\mathbf{r})$ is the chemical potential, and $\check{\Sigma}$ is the self-energy. Here the $U(\mathbf{r})$ is the interface potential including spin-flip scattering, which is expressed as the following spin dependent delta function in spin and particle-hole space.

$$U(\mathbf{r}) = \delta(z) (V_0 \rho_0 \sigma_0 + V_x \rho_0 \sigma_x + V_y \rho_z \sigma_y + V_z \rho_0 \sigma_z). \quad (\text{A2})$$

ρ_i and σ_i is Pauli matrix in particle-hole space, and in spin space, respectively. For the convenience, we consider V_0 and V_x only for potential scattering and spin-flip scattering, respectively, and ignore the other terms without loss of generality. Now we separate the above Green's

function into fast varying part and slow varying part on z .

$$\begin{aligned} \check{\mathbf{G}}(z, z'; \rho, i\omega_n) &= \check{G}_{11}(z, z'; \rho, i\omega_n) e^{ip_z(z-z')} \\ &+ \check{G}_{22}(z, z'; \rho, i\omega_n) e^{-ip_z(z-z')} \\ &+ \check{G}_{12}(z, z'; \rho, i\omega_n) e^{ip_z(z+z')} \\ &+ \check{G}_{21}(z, z'; \rho, i\omega_n) e^{-ip_z(z+z')} \end{aligned} \quad (\text{A3})$$

Now \check{G}_{ij} is the slowly varying function of z and z' . If we substitute Eq. (A1) by Eq. (A3) and neglect the second order derivatives, we get the equation for \check{G}_{ij} .

$$\left[-i\rho_z \omega_n - (-1)^k i v_{z1} \frac{\partial}{\partial z} + \frac{i}{2} \mathbf{v}_{\parallel} \frac{\partial}{\partial \rho} + \check{\Delta}(\mathbf{r}) - \check{\Sigma} \right] \check{G}_{kn}(z, z'; \rho, i\omega_n) = 0, \quad (z \neq z') \quad (\text{A4})$$

Here, we assume the z -direction is normal to the interface of the two region and ρ is the coordinates normal to the z -direction. We assume the translational symmetry in ρ -direction, and also assume that the boundary is sharp and plane. When $z, z' > 0$, v_{z1} is replaced by v_{z2} . The function \check{G}_{ij} 's for $z < z'$ and $z > z'$ are matched by

$$\check{G}_{kn}(z'+0, z') - \check{G}_{kn}(z'-0, z') = (-1)^k \frac{i}{\hbar v_{z1(2)}} \delta_{kn}. \quad (\text{A5})$$

To make the equations simpler, we introduce \hat{g} and \hat{G}

which are continuous at $z = z'$.

$$\begin{aligned} \hat{g}(z, z') &= 2i|v_{zj}| \begin{cases} \check{G}_{11}(z, z') - \text{sgn}(z - z'), & p_{zj} > 0, \\ \check{G}_{22}(z, z') + \text{sgn}(z - z'), & p_{zj} < 0, \end{cases} \\ \hat{G}(z, z') &= 2i|v_{zj}| \begin{cases} \check{G}_{12}(z, z'), & p_{zj} > 0, \\ \check{G}_{21}(z, z'), & p_{zj} < 0. \end{cases} \end{aligned} \quad (\text{A6})$$

For $z \ll z^* \equiv \min(l_j, v_{Fj}/\bar{\varepsilon}, a)$, we can write the equation for the Green's function using the fact that $\frac{\partial \check{\mathbf{G}}}{\partial \tau} \sim \frac{\partial \check{\mathbf{G}}}{\partial \tau'} \sim \bar{\varepsilon} \check{\mathbf{G}}$, where $\bar{\varepsilon} \sim \max(T, \Delta, V, \omega)$ as done by Zaitsev²⁹. The

equation for Green's function $\check{\mathbf{G}}$ is reduced to

$$H(z)\hat{\mathbf{G}}(z, z') = H(z')\hat{\mathbf{G}}(z, z') = \hat{0}, \quad (\text{A7})$$

where

$$H(z) \equiv \frac{\hbar^2}{2m} \frac{\partial^2}{\partial z^2} - U(z, \rho) + \mu - \frac{p_{\parallel}^2}{2m} \quad (\text{A8})$$

for $z \neq z'$. The solution can be written as

$$\check{\mathbf{G}} = A_{\pm}^{(j)} e^{ip_z(z-z')} + \bar{A}_{\pm}^{(j)} e^{-ip_z(z-z')} + B^{(j)} e^{ip_z(z+z')} + \bar{B}^{(j)} e^{ip_z(z+z')}, \quad (zz' > 0) \quad (\text{A9})$$

$$\check{\mathbf{G}} = A^{(jk)} e^{ip_z(z-z')} + \bar{A}^{(jk)} e^{-ip_z(z-z')} + B^{(jk)} e^{ip_z(z+z')} + \bar{B}^{(jk)} e^{ip_z(z+z')}, \quad (zz' < 0) \quad (\text{A10})$$

where the superscript $j, k = 1(2)$ denote the index of the region $z < -\delta$ ($z > \delta$), and the index $+(-)$ corresponds to $z > z'$ ($z < z'$). Now the above Green's functions can be written down by using the two linearly independent solution of the Schrödinger equation $H(z)\psi_{1,2}(z) = 0$.

$$\psi_1 = \begin{cases} e^{ip_{z1}z} + \check{r}e^{-ip_{z1}z}, & (z < 0) \\ \check{d}e^{ip_{z2}z}, & (z > 0) \end{cases} \quad (\text{A11})$$

$$\psi_2 = \begin{cases} \frac{p_{z1}}{p_{z2}} \check{d}e^{ip_{z2}z}, & (z < 0) \\ e^{ip_{z1}z} - \check{r}^\dagger \frac{\check{d}}{\check{d}^\dagger} e^{-ip_{z1}z}, & (z > 0) \end{cases} \quad (\text{A12})$$

where \check{r} and \check{d} is the spin dependent coefficient. For the spin space, it will have the form,

$$\check{r} = \begin{bmatrix} \frac{p_{z1}^2 - V_x^2 - (p_{z2} + iV_0)^2}{(p_{z1} + p_{z2} + iV_0)^2 + V_x^2} & \frac{-2ip_{z1}V_x}{(p_{z1} + p_{z2} + iV_0)^2 + V_x^2} \\ \frac{-2ip_{z1}V_x}{(p_{z1} + p_{z2} + iV_0)^2 + V_x^2} & \frac{p_{z1}^2 - V_x^2 - (p_{z2} + iV_0)^2}{(p_{z1} + p_{z2} + iV_0)^2 + V_x^2} \end{bmatrix}, \quad (\text{A13})$$

$$\check{d} = \begin{bmatrix} \frac{2ip_{z1}(p_{z1} + p_{z2} + iV_0)}{(p_{z1} + p_{z2} + iV_0)^2 + V_x^2} & \frac{-2ip_{z1}V_x}{(p_{z1} + p_{z2} + iV_0)^2 + V_x^2} \\ \frac{-2ip_{z1}V_x}{(p_{z1} + p_{z2} + iV_0)^2 + V_x^2} & \frac{2ip_{z1}(p_{z1} + p_{z2} + iV_0)}{(p_{z1} + p_{z2} + iV_0)^2 + V_x^2} \end{bmatrix}. \quad (\text{A14})$$

For $|z|, |z'| \ll z^*$, $\check{\mathbf{G}}$ can be represented in the form,

$$\check{\mathbf{G}}(z, z') = \begin{cases} e^{ip_{z1}z'} F_1(z) + e^{-ip_{z1}z'} \bar{F}_1(z), & z' < -\delta, z > z' \\ e^{ip_{z2}z'} F_2(z) + e^{-ip_{z2}z'} \bar{F}_2(z), & z' > \delta, z < z' \\ e^{ip_{z1}z} P_1(z') + e^{-ip_{z1}z} \bar{P}_1(z'), & z < -\delta, z < z' \\ e^{ip_{z2}z} P_2(z') + e^{-ip_{z2}z} \bar{P}_2(z'), & z > \delta, z > z' \end{cases}, \quad (\text{A15})$$

where

$$F_i(z) = \psi_1(z) \cdot \mathbf{f}_{i1} + \psi_2(z) \cdot \mathbf{f}_{i2}, \quad (\text{A16})$$

$$P_i(z) = \psi_1(z) \cdot \mathbf{p}_{i1} + \psi_2(z) \cdot \mathbf{p}_{i2}, \quad (\text{A17})$$

Here, $\mathbf{f}_{i1(2)}$ and $\mathbf{p}_{i1(2)}$ are 4×4 matrix in spin and particle-hole space. The coefficients A_{\pm}^j, B^j, B^{jk} and \bar{B}^{jk} is related to the Green's function at the vicinity of the interface. For the relation between the Green's function of the region 1 and region 2 near the interface, we compare the solution of Eq. (A15) with Eqs. (A9) and (A10), then we can write down the coefficients A_{\pm}^j, B^j, B^{jk} and \bar{B}^{jk}

in terms of $\mathbf{f}_{i1(2)}$ and $\mathbf{p}_{i1(2)}$. If we eliminate the term $\mathbf{f}_{i1(2)}$ and $\mathbf{p}_{i1(2)}$, we get the following relations.

$$\begin{aligned} v_1 A_{\pm}^1 - v_2 A_{\pm}^2 &= v_1 \bar{A}_{\pm}^1 - v_2 \bar{A}_{\pm}^2 = \\ v_2 \frac{\hat{r} \hat{d}^\dagger}{\hat{d}} B^2 + v_1 \hat{r}^\dagger \bar{B}^1 &= v_1 \hat{r} B^1 + v_2 \frac{\hat{r}^\dagger \hat{d}}{\hat{d}^\dagger} \bar{B}^2, \quad (\text{A18}) \\ v_1 \bar{A}_{\pm}^1 + v_2 A_{\pm}^2 &= v_1 A_{\pm}^1 + v_2 \bar{A}_{\pm}^2 = \\ -v_2 \frac{\hat{d}^\dagger}{\hat{r}^\dagger \hat{d}} B^2 + v_1 \frac{1}{\hat{r}^\dagger} B^1 &= -v_2 \frac{\hat{d}}{\hat{r} \hat{d}^\dagger} \bar{B}^2 + v_1 \frac{1}{\hat{r}} \bar{B}^1 \quad (\text{A19}) \end{aligned}$$

Here, we define the function $\check{\mathcal{G}}$ from $\check{\mathbf{G}}$.

$$\check{\mathcal{G}} = \begin{cases} \hat{r} \check{\mathcal{G}} & z < -\delta, p_i > 0 \\ \hat{r}^\dagger \check{\mathcal{G}} & z < -\delta, p_i < 0 \\ \frac{\hat{r} \hat{d}^\dagger}{\hat{d}} \check{\mathcal{G}} & z > \delta, p_i > 0 \\ \frac{\hat{r}^\dagger \hat{d}}{\hat{d}^\dagger} \check{\mathcal{G}} & z > \delta, p_i < 0 \end{cases} \quad (\text{A20})$$

Now we define the symmetric and asymmetric component of the Green's function.

$$\check{g}_{s(a)} = \frac{\check{g}(p) \pm \check{g}(-p)}{2} \quad (\text{A21})$$

From the Eqs. (A9) and (A10), we get the following expression for $\check{g}_{s(a)}$ and $\check{\mathcal{G}}_{s(a)}$:

$$\begin{aligned} \check{g}_s &= iv_j (A_{\pm}^j + \bar{A}_{\pm}^j) \\ \check{g}_a &= iv_j (A_{\pm}^j - \bar{A}_{\pm}^j) - \text{sgn}(z - z') \\ \check{\mathcal{G}}_s &= \begin{cases} \frac{v_1}{2} (\hat{r} B^1 + \hat{r}^\dagger \bar{B}^1) & z, z' < -\delta \\ \frac{v_2}{2} \left(\frac{\hat{r} \hat{d}^\dagger}{\hat{d}} B^2 + \frac{\hat{r}^\dagger \hat{d}}{\hat{d}^\dagger} \bar{B}^2 \right) & z, z' > \delta \end{cases} \\ \check{\mathcal{G}}_a &= \begin{cases} \frac{v_1}{2} (\hat{r} B^1 - \hat{r}^\dagger \bar{B}^1) & z, z' < -\delta \\ \frac{v_2}{2} \left(\frac{\hat{r} \hat{d}^\dagger}{\hat{d}} B^2 - \frac{\hat{r}^\dagger \hat{d}}{\hat{d}^\dagger} \bar{B}^2 \right) & z, z' > \delta \end{cases} \quad (\text{A22}) \end{aligned}$$

From the relation Eqs. (A18), (A19), and (A22), we get the relations for the symmetric and the asymmetric Green's function.

$$\check{g}_a^{(1)} = \check{g}_a^{(2)} = \check{g}_a \quad (\text{A23})$$

$$\check{\mathcal{G}}_a^{(1)} = \check{\mathcal{G}}_a^{(2)} = \check{\mathcal{G}}_a \quad (\text{A24})$$

$$\check{g}_s^{(1)} - \check{g}_s^{(2)} = \check{\mathcal{G}}_s^{(1)} + \check{\mathcal{G}}_s^{(2)} \quad (\text{A25})$$

$$\check{g}_s^{(1)} + \check{g}_s^{(2)} = \frac{1}{R} (\check{\mathcal{G}}_s^{(1)} - \check{\mathcal{G}}_s^{(2)}) \quad (\text{A26})$$

Here, R is reflection coefficient. The reflection and transmission coefficient are

$$D = \frac{p_{z2}}{p_{z1}} \hat{d}^\dagger \hat{d}, \quad R = \hat{r}^\dagger \hat{r} = 1 - D. \quad (\text{A27})$$

For the derivation of the boundary conditions in terms of \check{g} only, we use the following relation.

$$\check{g} \check{\mathcal{G}} = (-1)^j \text{sgn} p_j \check{\mathcal{G}} \quad (\text{A28})$$

For the proof of the above relation, the readers refer to Zaitsev²⁹. By using (A28), we get the following relations.

$$\begin{aligned} \check{g}_s \check{\mathcal{G}}_s + \check{g}_a \check{\mathcal{G}}_a &= (-1)^j \check{\mathcal{G}}_a, \\ \check{g}_s \check{\mathcal{G}}_a + \check{g}_a \check{\mathcal{G}}_s &= (-1)^j \check{\mathcal{G}}_s. \end{aligned} \quad (\text{A29})$$

Using the above equations with Eqs. (A23), (A24), (A25), and (A26), we eliminate $\check{\mathcal{G}}_s$ and get the following relations.

$$-\check{g}_s^+ R \check{g}_s^+ - (\check{g}_s^-)^2 = \check{\mathcal{G}}_a, \quad (\text{A30})$$

$$\check{g}_s^+ \check{g}_s^- + \check{g}_s^- R \check{g}_s^+ = \check{g}_a \check{\mathcal{G}}_a, \quad (\text{A31})$$

$$\check{g}_s^+ \check{\mathcal{G}}_a - \check{g}_a \check{g}_s^- = -R \check{g}_s^+, \quad (\text{A32})$$

$$\check{g}_s^- \check{\mathcal{G}}_a - \check{g}_a R \check{g}_s^+ = -\check{g}_s^-, \quad (\text{A33})$$

where we introduce

$$\check{g}_s^\pm = \frac{\check{g}^{(1)} \pm \check{g}^{(2)}}{2}. \quad (\text{A34})$$

From these four relations, we again eliminate $\check{\mathcal{G}}_a$ and we get

$$\check{g}_s^+ (\check{g}_s^-)^3 + \check{g}_a (\check{g}_s^-)^2 = \left\{ 1 - (\check{g}_s^+)^2 \right\} R \check{g}_s^+ \check{g}_s^- \quad (\text{A35})$$

$$(\check{g}_s^-)^3 \check{g}_s^+ + \check{g}_a R (\check{g}_s^+)^2 = \check{g}_s^- \check{g}_s^+ \left\{ 1 - R (\check{g}_s^+)^2 \right\} \quad (\text{A36})$$

By considering the following commutation relations,

$$[\check{g}_s^+, \check{g}_s^-]_+ = \check{0}, \quad \text{and} \quad [\check{g}_s^\pm, \check{g}_a]_+ = \check{0}, \quad (\text{A37})$$

finally, with Eq. (A23), we get the following two boundary conditions in terms of \check{g} only.

$$\check{g}_a^{(2)} - \check{g}_a^{(1)} = 0, \quad (\text{A38})$$

$$\begin{aligned} \check{g}_a \left[\check{R} (\check{g}_s^+)^2 + (\check{g}_s^-)^2 \right] &= D \check{g}_s^- \check{g}_s^+ \quad (\text{A39}) \\ &\quad - \left[R \check{g}_s^- \check{g}_s^+, (\check{g}_s^+)^2 \right]_-. \end{aligned}$$

This is the new boundary condition for the Eilenberger equation with spin-flip scattering at the interface.

APPENDIX B: BOUNDARY CONDITIONS FOR USADEL EQUATION

For the case without spin-flip scattering at the interface, The boundary conditions for the Usadel equation is derived from the Eilenberger equations by Kuprianov *et al.*³⁰ in the vicinity of interface within the mean free path ℓ . We will use the same methods and assumptions of Kuprianov *et al.* for deriving the boundary condition of Usadel equation from that of Eilenberger equation which we derived in Appendix A for spin-flip scattering at the interface. The boundary condition is directly connected to the continuity of the normal and anomalous Green's

functions of Eilenberger equation. In the Eilenberger equation, if we neglect terms of ω and Δ , we get

$$2\ell_i \cdot \nabla \check{g}_a^i = \check{g}_s^i \langle \check{g}_s^i \rangle - \langle \check{g}_s^i \rangle \check{g}_s^i \quad (\text{B1})$$

$$2\ell_i \cdot \nabla \check{g}_s^i = \check{g}_a^i \langle \check{g}_s^i \rangle - \langle \check{g}_s^i \rangle \check{g}_a^i \quad (\text{B2})$$

where \check{g} is the quasi-classical Green's function in Nambu-Gor'kov space.

$$\check{g} = 2\pi N(0) \begin{bmatrix} i\hat{g} & \hat{f} \\ \hat{f}^\dagger & -i\hat{g} \end{bmatrix}, \quad (\text{B3})$$

with normal and anomalous Green's function in spin space,

$$\hat{g} = \begin{bmatrix} g_{\uparrow\uparrow} & g_{\uparrow\downarrow} \\ g_{\downarrow\uparrow} & g_{\downarrow\downarrow} \end{bmatrix}, \quad \text{and} \quad \hat{f} = \begin{bmatrix} f_{\uparrow\uparrow} & f_{\uparrow\downarrow} \\ f_{\downarrow\uparrow} & f_{\downarrow\downarrow} \end{bmatrix} \quad (\text{B4})$$

Here, the brackets imply an integration over the solid angles, $\langle \dots \rangle = \int d\Omega/4\pi$. The superscript i in Eqs. (B1) and (B2) stands for the region index as j and k in Eqs. (A9) and (A10). Far from the boundary, the isotropic Usadel function²⁶ is identified as \check{g}_s , and \check{g}_a can be also written in terms of Usadel function.

$$\check{g}_s^i = \langle \check{g}_s^i \rangle = \check{G}_i, \quad \check{g}_a^i = \ell \cdot (\check{G}_i \nabla \check{G}_i), \quad (\text{B5})$$

where

$$\check{G} = \begin{bmatrix} i\hat{G} & \hat{F} \\ \hat{F}^\dagger & -i\hat{G} \end{bmatrix}. \quad (\text{B6})$$

The derivation of the boundary condition of the Usadel equation for the derivatives of the Usadel function from the first boundary condition of Eilenberger equation, (A38), is the exactly same as that of Kuprianov *et al.*³⁰. Therefore, we get the following boundary condition for the derivative of the anomalous function in Usadel equation.

$$\xi_1 \frac{\partial}{\partial z} \hat{F}_1 = \gamma \xi_2 \frac{\partial}{\partial z} \hat{F}_2, \quad \gamma \equiv \frac{\rho_1 \xi_1}{\rho_2 \xi_2} \quad (\text{B7})$$

For the second boundary condition, we assume $R \cdot \hat{1} \gg D(\check{g}_s^-)^2$, and $R(\check{g}_a)^2$ is neglected. From Eq. (B5), we have $\check{g}_a^i \ll \check{g}_s^i$ far enough from the boundary. With the help of the relation $\check{g}_a^2 + \check{g}_s^2 = \hat{1}$, we simplify the Eq. (A39).

$$\check{g}_a R = \check{g}_s^- \check{g}_s^+ D \quad (\text{B8})$$

From the relation between Usadel function and Eilenberger function, Eq. (B5), we rewrite Eq. (B8) in terms of Usadel function.

$$\ell_2 \check{G}_2 \nabla \check{G}_2 \frac{4}{3} \left\langle \frac{x_2 R}{D} \right\rangle = \check{G}_2 \check{G}_1 - \check{G}_1 \check{G}_2 \quad (\text{B9})$$

For the boundary condition of anomalous Usadel function, we write the Eq. (B9) in terms of normal and anomalous Usadel function by using Eq. (B6).

$$\frac{4}{3} \ell_2 \hat{G}_2 \nabla \hat{F} \left\langle \frac{x_2 R}{D} \right\rangle = [\hat{G}_2, \hat{F}_1 - \hat{F}_2]_+ + [\hat{G}_1, \hat{F}_1 - \hat{F}_2]_+ \quad (\text{B10})$$

At T_C , the normal Usadel function can be expressed as the following form which is derived in Appendix C.

$$\hat{G}_{1(2)} = (\hat{1} + \text{Re} \langle \hat{r} \rangle) \text{sgn}(\omega) + i \text{Im} \langle \hat{r} \rangle, \quad (\text{B11})$$

Now we substitute (B11) into (B10), the boundary condition for the anomalous Green's function will be

$$\xi_2(1 + \text{Re} \hat{r} + i \text{sgn}(\omega) \text{Im} \hat{r}) \nabla \hat{F}_2 \gamma_B = \hat{F}_1 - \hat{F}_2 + [\text{Re} \hat{r} + i \text{sgn} \omega \text{Im} \hat{r}, \hat{F}_1 - \hat{F}_2]_+, \quad (\text{B12})$$

where

$$\gamma_B = \frac{2 \ell_2}{3 \xi_2} \left\langle \frac{x_2 R}{D} \right\rangle. \quad (\text{B13})$$

Here the anomalous Usadel function is 2×2 matrix in the spin space. This can be represented in the form of spin-singlet and triplet components.

$$\hat{F}(\omega) = i \sigma_y F_s(+) + \sigma_x F_{tx}(-) + \sigma_z F_{tz}(-) + \sigma_0 F_{t0}(-) \quad (\text{B14})$$

where

$$F_s \equiv \frac{F_{\uparrow\downarrow} - F_{\downarrow\uparrow}}{2}, \quad F_{tx} \equiv \frac{F_{\uparrow\downarrow} + F_{\downarrow\uparrow}}{2}, \\ F_{tz} \equiv \frac{F_{\uparrow\uparrow} - F_{\downarrow\downarrow}}{2}, \quad \text{and} \quad F_{t0} \equiv \frac{F_{\uparrow\uparrow} + F_{\downarrow\downarrow}}{2}, \quad (\text{B15})$$

and the plus and minus sign means even and odd function in the frequency space.

$$F_\alpha(\pm) = \frac{F_\alpha(\omega) \pm F_\alpha(-\omega)}{2}, \quad (\alpha = s, tx, tz, \text{ and } t0) \quad (\text{B16})$$

In vector notation of the anomalous Usadel function we have the following form of the second boundary condition.

$$\mathcal{F}_1 - \mathcal{F}_2 = \hat{\gamma}_b \xi_2 \nabla \mathcal{F}_2, \quad (\text{B17})$$

where

$$\mathcal{F} \equiv \begin{bmatrix} F_s(+) \\ F_{tx}(-) \\ F_{tz}(-) \\ F_{t0}(-) \end{bmatrix}, \quad \text{and} \quad \hat{\gamma}_b = \begin{bmatrix} \gamma_1 & 0 & \gamma_2 & 0 \\ 0 & \gamma_3 & 0 & \gamma_4 \\ \gamma_2 & 0 & \gamma_1 & 0 \\ 0 & \gamma_4 & 0 & \gamma_3 \end{bmatrix} \quad (\text{B18})$$

Since we expressed the spin-dependent interfacial potential in terms of σ_0 and σ_x , the following quantities are also expressed as

$$\langle r \rangle = r_0 \sigma_0 + r_x \sigma_x, \quad \left\langle \frac{2 x_2 R}{3 D} \right\rangle = \gamma_0 \sigma_0 + \gamma_x \sigma_x. \quad (\text{B19})$$

Therefore the γ_i 's in (B18) can be expressed as

$$\gamma_1 = \frac{1}{2} \left(\gamma_0 - \frac{\gamma_x \text{Re} r_x}{1 + \text{Re} r_0} \right), \quad \gamma_3 = \frac{\gamma_0}{2}, \quad (\text{B20})$$

$$\gamma_2 = \frac{i \gamma_x \text{Im} r_0 - \gamma_0 \text{Im} r_x}{2(1 + \text{Re} r_0)}, \quad \gamma_4 = \frac{\gamma_x}{2}. \quad (\text{B21})$$

If we compare the result of Kuprianov when $r_x = 0$, we get

$$\gamma_0 = \frac{R_b \mathcal{A}}{\xi_2 \rho_2} \equiv \gamma_b \quad (\text{B22})$$

When the interface potential V_0 and V_x are small, and if we ignore the higher terms of V_0 and V_x , the parameters in terms of the lowest order of V_0 and V_x .

$$\gamma_1 \approx \gamma_b + \mathcal{O}(V_0^2 V_x^2), \quad \gamma_3 \approx \gamma_b, \\ \gamma_2 \approx i \frac{V_x}{p_{F1} + p_{F2}} \equiv i \gamma_m, \quad \gamma_4 \approx \mathcal{O}(V_x^2) \quad (\text{B23})$$

Finally, the two boundary condition for the Usadel functions are

$$\xi_1 \nabla \mathcal{F}_1 = \gamma \xi_2 \nabla \mathcal{F}_2, \quad \gamma = \frac{\rho_1 \xi_1}{\rho_2 \xi_2} \quad (\text{B24})$$

$$\mathcal{F}_1 - \mathcal{F}_2 = \hat{\gamma}_b \xi_2 \nabla \mathcal{F}_2, \quad \hat{\gamma}_b \approx \begin{bmatrix} \gamma_b & 0 & i \gamma_m & 0 \\ 0 & \gamma_b & 0 & 0 \\ i \gamma_m & 0 & \gamma_b & 0 \\ 0 & 0 & 0 & \gamma_b \end{bmatrix}.$$

APPENDIX C: DERIVATION FOR THE NORMAL USADEL FUNCTION AT T_C

In this section, we will derive the Usadel function of normal Green's function at T_C \hat{G} of Eq. (B11) in Appendix B. Without any spin-flip scattering at the interface, \hat{G} is simply as following.

$$\hat{G} = \text{sgn} \omega \quad \text{for } V_x = 0. \quad (\text{C1})$$

To get the expression for \hat{G} with spin-flip scattering, $V_x \neq 0$. We start from the eigen function of the Hamiltonian (A8),

$$\hat{\phi}_+(x) = \frac{1}{\sqrt{2\pi}} \begin{cases} (e^{ip_1 x} + \hat{r} e^{-ip_1 x}) & (x < 0) \\ d e^{ip_2 x} & (x > 0) \end{cases}, \quad (\text{C2})$$

$$\hat{\phi}_-(x) = \frac{\sqrt{p_1/p_2}}{\sqrt{2\pi}} \begin{cases} \frac{p_2}{p_1} d e^{-ip_1 x} & (x < 0) \\ (e^{-ip_2 x} - \hat{r}^\dagger \frac{d}{d^\dagger} e^{ip_2 x}) & (x > 0) \end{cases} \quad (\text{C3})$$

Now, we derive the normal Usadel function from the following definition of the Green's function.

$$\hat{G} = \frac{i}{N(0)} \sum_p \begin{cases} \frac{\hat{\phi}_+(z_1) \hat{\phi}_+^\dagger(z_2) + \hat{\phi}_-(z_1) \hat{\phi}_-^\dagger(z_2)}{i\omega - \epsilon} & (\epsilon > 0) \\ \frac{\hat{\phi}_+^\dagger(z_1) \hat{\phi}_+(z_2) + \hat{\phi}_-^\dagger(z_1) \hat{\phi}_-(z_2)}{i\omega - \epsilon} & (\epsilon < 0) \end{cases} \quad (\text{C4})$$

Here $N(0)$ is the density of state at Fermi level. For the simplicity, we will deal with one-dimensional case. If we write down in terms of the center of mass and relative coordinate, we have the following form:

$$\begin{aligned}
\hat{G} = & \frac{i}{N(0)} \sum_p \frac{e^{i(P+p)z} + e^{-i(P+p)z} + \hat{r}^\dagger e^{i(P+p)Z} + \hat{r} e^{-i(P+p)Z}}{i\omega - \epsilon} \theta(Z < z < -Z) \theta(-Z) \theta(\epsilon) \\
& + \frac{e^{-i(P+p)z} + e^{i(P+p)z} + \hat{r}^\dagger e^{i(P+p)Z} + \hat{r} e^{-i(P+p)Z}}{i\omega - \epsilon} \theta(Z < z < -Z) \theta(-Z) \theta(-\epsilon) \\
& + \frac{p_1 e^{-i(P-p)z} + e^{i(P-p)z} - \hat{r}^\dagger \frac{\hat{d}}{\hat{d}^\dagger} e^{i(P-p)Z} - \hat{r} \frac{\hat{d}^\dagger}{\hat{d}} e^{-i(P-p)Z}}{i\omega - \epsilon} \theta(-Z < z < Z) \theta(Z) \theta(\epsilon) \\
& + \frac{p_1 e^{i(P-p)z} + e^{-i(P-p)z} - \hat{r}^\dagger \frac{\hat{d}}{\hat{d}^\dagger} e^{i(P-p)Z} - \hat{r} \frac{\hat{d}^\dagger}{\hat{d}} e^{-i(P-p)Z}}{i\omega - \epsilon} \theta(-Z < z < Z) \theta(Z) \theta(-\epsilon) \\
& + \frac{\hat{d} e^{-i(pZ+Pz)} + \hat{d}^\dagger e^{i(pZ+Pz)}}{i\omega - \epsilon} (\theta(Z) \theta(z < -Z) + \theta(-Z) \theta(z < Z)) \\
& + \frac{\hat{d} e^{-i(pZ-Pz)} + \hat{d}^\dagger e^{i(pZ-Pz)}}{i\omega - \epsilon} (\theta(Z) \theta(z > Z) + \theta(-Z) \theta(z > -Z))
\end{aligned}$$

At the boundary $Z = 0$, we get

$$\hat{G}(k_z, \omega, Z = 0) = \frac{i}{N(0)} \int_{-\infty}^{\infty} dz \sum_P \text{Re} \hat{d} \frac{e^{iPz} + e^{-iPz}}{i\omega - \epsilon} + i \text{Im} \hat{d} \frac{e^{iPz} - e^{-iPz}}{i\omega - \epsilon} \text{sgn } z \quad (\text{C5})$$

After integration over z and P , we have the normal Usadel function with spin-flip scattering at the interface,

$$\hat{G}(k_z, \omega, Z = 0) = (1 + \text{Re} \langle \hat{r} \rangle) \text{sgn}(\omega) + i \text{Im} \langle \hat{r} \rangle, \quad (\text{C6})$$

Without any reflection at the interface, Eq. (C6) is reduced to Eq. (C1). The imaginary part in Eq. (C6) has key role to give a coupling term between singlet pairing state of even function in frequency and triplet pairing state of odd function in frequency.

APPENDIX D: CALCULATION OF T_C

In this section, we will get the T_C equation of a S/F bilayer by solving Eqs. (17), (18), (20), (21), and (22). The triplet pairing components of \mathcal{F}^S of Eq. (18) satisfy the homogeneous equation unlike the singlet pairing component which has inhomogeneous term $\Delta(x)$. Therefore, the solutions of triplet components in Eq. (17) with the boundary condition (20) can be written down easily as follows.

$$F_{t\alpha}^S(x) = C_{t\alpha}^S \cosh k_S(x - d_S), \quad (\alpha = x, z, \text{ and } 0) \quad (\text{D1})$$

with

$$k_S = \frac{1}{\xi_S} \sqrt{\frac{|\omega_n|}{\pi T_C}}. \quad (\text{D2})$$

In the ferromagnetic region, Eq. (18) is also homogeneous equation, and easily solved. The solutions of \mathcal{F}^F in Eq.

(18) with the boundary condition (20) are

$$\mathcal{F}^F(x) = \begin{bmatrix} c_F(x) & c_F^*(x) & 0 & 0 \\ -c_F(x) & c_F^*(x) & 0 & 0 \\ 0 & 0 & c_F^0(x) & 0 \\ 0 & 0 & 0 & c_F^0(x) \end{bmatrix} \begin{bmatrix} C_s^F \\ C_t^F \\ C_t^F \\ C_{t0}^F \end{bmatrix}, \quad (\text{D3})$$

where

$$c_F(x) = \cosh k_F(x + d_F), \quad (\text{D4})$$

$$c_F^0(x) = \cosh k_F^0(x + d_F), \quad (\text{D5})$$

with

$$k_F = \frac{1}{\xi_F} \sqrt{\frac{|\omega_n| + i\hbar_z}{\pi T_C}}, \quad \text{and } k_F^0 = \frac{1}{\xi_F} \sqrt{\frac{|\omega_n|}{\pi T_C}}. \quad (\text{D6})$$

F_s^S , the singlet pairing component of the vector \mathcal{F}^S , satisfies the inhomogeneous equation (17), but the others, the triplet pairing components, do the homogeneous equation. So, it is useful to define projection operators to distinguish the two group.

$$\mathcal{P}_s = \begin{bmatrix} 1 & 0 & 0 & 0 \\ 0 & 0 & 0 & 0 \\ 0 & 0 & 0 & 0 \\ 0 & 0 & 0 & 0 \end{bmatrix}, \quad \mathcal{P}_t = \begin{bmatrix} 0 & 0 & 0 & 0 \\ 0 & 1 & 0 & 0 \\ 0 & 0 & 1 & 0 \\ 0 & 0 & 0 & 1 \end{bmatrix}. \quad (\text{D7})$$

Here, the subscript s denotes as singlet, and t as triplet. At $x = 0$, from the solutions (D1) and (D3), we get the following relations,

$$\mathcal{P}_t \xi_S \frac{\partial}{\partial x} \mathcal{F}^S(0) = -A_S \mathcal{P}_t \mathcal{F}^S(0), \quad \text{and} \quad (\text{D8})$$

$$\mathcal{F}^F(0) = \hat{B}_F \xi_F \frac{\partial}{\partial x} \mathcal{F}^F(0), \quad (\text{D9})$$

respectively, with

$$A_S = k_S \xi_S \tanh k_S d_S, \quad \text{and} \quad (\text{D10})$$

$$\hat{B}_F = \begin{bmatrix} \text{Re}B_F & -i\text{Im}B_F & 0 & 0 \\ -i\text{Im}B_F & \text{Re}B_F & 0 & 0 \\ 0 & 0 & B_{F0} & 0 \\ 0 & 0 & 0 & B_{F0} \end{bmatrix}, \quad (\text{D11})$$

where

$$B_F = [k_F \xi_F \tanh k_F d_F]^{-1}, \quad \text{and} \quad (\text{D12})$$

$$B_{F0} = [k_F^0 \xi_F \tanh k_F^0 d_F]^{-1}. \quad (\text{D13})$$

From Eqs. (D9), (21), and (22), we get the coupled boundary condition for \mathcal{F}^S at $x = 0$.

$$\xi_S \frac{\partial}{\partial x} \mathcal{F}^S(0) = \hat{A} \mathcal{F}^S(0), \quad (\text{D14})$$

where

$$\hat{A} = \frac{\gamma \hat{I}}{\hat{B}_F + \hat{\gamma}_b}. \quad (\text{D15})$$

Since $\mathcal{P}_s + \mathcal{P}_t$ is identity operator, the following should be satisfied.

$$(\mathcal{P}_s + \mathcal{P}_t) \xi_S \frac{\partial}{\partial x} \mathcal{F}^S(0) = (\mathcal{P}_s + \mathcal{P}_t) \hat{A} (\mathcal{P}_s + \mathcal{P}_t) \mathcal{F}^S(0). \quad (\text{D16})$$

By utilizing (D8) and (D14), we can derive the boundary relation between $\frac{\partial}{\partial x} F_s^S(0)$ and $F_s^S(0)$. The boundary condition for the singlet component at the S region is

$$\xi_S \frac{\partial}{\partial x} F_s^S(0) = W(\omega_n) F_s^S(0), \quad (\text{D17})$$

where

$$W = \frac{\gamma [\gamma + A_S (\text{Re}B_F + \gamma_b)]}{A_S |B_F + \gamma_b|^2 + \gamma (\text{Re}B_F + \gamma_b) + A_S \gamma_m^2 \kappa}, \quad (\text{D18})$$

$$\kappa = \frac{\gamma + A_S (\text{Re}B_F + \gamma_b)}{\gamma + A_S (B_{F0} + \gamma_b)}.$$

Here, we reduce the three component inhomogeneous difference equation to the single component inhomogeneous differential equation for $F_s^S(x, i\omega_n)$, which satisfies (D17) and

$$\pi T_C \xi_S^2 \frac{\partial^2}{\partial x^2} F_s^S(x, i\omega_n) - |\omega_n| F_s^S(x, i\omega_n) = -2\Delta(x) \quad (\text{D19})$$

from Eq. (17).

To solve the inhomogeneous equation, we have to solve the following source equation.

$$\pi T_C \xi_S^2 \frac{\partial^2}{\partial x^2} G(x, y) - |\omega| G(x, y) = -\delta(x - y). \quad (\text{D20})$$

With the boundary condition (D17) and (20), we have

$$\xi_S \frac{\partial}{\partial x} G(0, y) = W(\omega_n) G(0, y), \quad (\text{D21})$$

$$\xi_S \frac{\partial}{\partial x} G(d_s, y) = 0. \quad (\text{D22})$$

The solution of Eqs. (D20), (D21), and (D22) has the following form.

$$G(x, y, i\omega_n) = \frac{k_S / |\omega_n|}{\sinh k_S d_s + \frac{W(\omega_n)}{k_S \xi_S} \cosh k_S d_s} \times \begin{cases} v_1(x) v_2(y), & 0 < x < y \\ v_1(y) v_2(x), & y < x < d_s \end{cases} \quad (\text{D23})$$

where

$$v_1(x) = \cosh k_S x + \frac{W(\omega_n)}{k_S \xi_S} \sinh k_S x, \quad (\text{D24})$$

$$v_2(x) = \cosh k_S (x - d_s). \quad (\text{D25})$$

Now, the solution of Eq. (D19) is

$$F_s^S(x, i\omega_n) = 2 \int_0^{d_s} dy G(x, y, i\omega_n) \Delta(y). \quad (\text{D26})$$

Since the order parameter $\Delta(x)$ is determined by the symmetric part of the anomalous function F_s^S , the self-consistency equation comes from

$$\Delta(x) = \pi T_C \lambda g(\epsilon_F) \sum_{\omega_n > 0} F_s^S(x, i\omega_n). \quad (\text{D27})$$

Substituting (D26) into (D27) gives the self-consistency equation,

$$\Delta(x) = 2\pi T_C \lambda g(\epsilon_F) \sum_{\omega_n > 0} \int_0^{d_s} dy G(x, y, i\omega_n) \Delta(y). \quad (\text{D28})$$

From this self-consistency equation, we can write down the equation for T_C with respect to the bulk transition temperature T_{C0} .

$$\Delta(x) \ln \frac{T_{C0}}{T_C} \quad (\text{D29})$$

$$= 2\pi T_C \sum_{\omega_n > 0} \int_0^{d_s} dy \left(\frac{\delta(x-y)}{|\omega_n|} - G(x, y, i\omega_n) \right) \Delta(y)$$

The above integral equation in (D29) can be reduced to an eigenvalue problem after we change the integration for the function $G(x, y)$ over y into summation over discrete y . The integral domain y is divided into N grids, and we change the integration over y into the following summation to obtain Eq. (24) in Sec. II.

$$\Delta_n \ln \frac{T_{C0}}{T_C} = \sum_m^N K_{nm} \Delta_m \quad (\text{D30})$$

where we define

$$\Delta_n \equiv \Delta \left(\frac{d_S}{N} n \right) \quad (\text{D31})$$

$$K_{nm} \equiv 2\pi T_C \sum_{\omega_n > 0} \left(\frac{\delta_{nm}}{|\omega_n|} - G_{nm}(i\omega_n) \right) \quad (\text{D32})$$

$$G_{nm}(i\omega) \equiv G \left(\frac{d_S}{N} n, \frac{d_S}{N} m, i\omega_n \right). \quad (\text{D33})$$

The T_C is determined by the smallest eigenvalue which gives the largest T_C .

-
- * Electronic address: clotho@phys1.skku.ac.kr
† Electronic address: hychoi@skku.ac.kr
- ¹ N. R. Werthamer, *Phys. Rev.* **132**, 2440 (1963).
² P. G. de Gennes, *Rev. Mod. Phys.* **36**, 225 (1964).
³ P. Fulde and A. Ferrel, *Phys. Rev.* **135**, A550 (1964).
⁴ A. Larkin and Y. Ovchinnikov, *Sov. Phys. JETP* **20**, 762 (1965).
⁵ L. N. Bulaevskii and V. V. Kuzii, *Sov. J. Low Temp. Phys.* **3**, 352 (1977).
⁶ A. I. Buzdin, L. N. Bulaevskii, and S. V. Panyukov, *JETP Lett.* **35**, 178 (1982).
⁷ A. I. Buzdin and M. Y. Kupriyanov, *JETP Lett.* **52**, 487 (1990).
⁸ A. I. Buzdin and M. Y. Kupriyanov, *JETP Lett.* **53**, 321 (1991).
⁹ J. S. Jiang, D. Davidovic, D. H. Reich, and C. L. Chien, *Phys. Rev. Lett.* **74**, 314 (1995).
¹⁰ T. Mühge, N. N. Garif'yanov, Y. V. Goryunov, G. G. Khal-iullin, L. R. Tagirov, K. Westerholt, I. A. Garifullin, and H. Zabel, *Phys. Rev. Lett.* **77**, 1857 (1996).
¹¹ T. Kontos, M. Aprili, J. Lesueur, and X. Grison, *Phys. Rev. Lett.* **86**, 304 (2001).
¹² V. V. Ryazanov, V. A. Oboznov, A. Y. Rusanov, A. V. Veretennikov, A. A. Golubov, and J. Aarts, *Phys. Rev. Lett.* **86**, 2427 (2001).
¹³ T. Kontos, M. Aprili, J. Lesueur, F. Genet, B. Stephanidis, and R. Boursier, *Phys. Rev. Lett.* **89**, 137007 (2002).
¹⁴ W. Guichard, M. Aprili, O. Bourgeois, T. Kontos, J. Lesueur, and P. Gandit, *Phys. Rev. Lett.* **90**, 167001 (2003).
¹⁵ M. Giroud, H. Courtois, K. Hasselbach, D. Mailly, and B. Pannetier, *Phys. Rev. B* **58**, R11872 (1998).
¹⁶ V. T. Petrashov, I. A. Sosnin, I. Cox, A. Parsons, and C. Troadec, *Phys. Rev. Lett.* **83**, 3281 (1999).
¹⁷ J. Y. Gu, C.-Y. You, J. S. Jiang, J. Pearson, Y. B. Bazaliy, and S. D. Bader, *Phys. Rev. Lett.* **89**, 267001 (2002).
¹⁸ E. A. Demler, G. G. Arnold, and M. R. Beasley, *Phys. Rev. B* **55**, 15174 (1997).
¹⁹ F. S. Bergeret, A. F. Volkov, and K. B. Efetov, *Phys. Rev. Lett.* **86**, 4096 (2001).
²⁰ V. M. Edelstein, *JETP Lett.* **77**, 182 (2003).
²¹ M. Eschrig, J. Kopu, J. C. Cuevas, and G. Schön, *Phys. Rev. Lett.* **90**, 137003 (2003).
²² A. F. Volkov, F. S. Bergeret, and K. B. Efetov, *Phys. Rev. Lett.* **90**, 117006 (2003).
²³ Y. V. Fominov, A. A. Golubov, and M. Y. Kupriyanov, *JETP Lett.* **77**, 510 (2003).
²⁴ F. S. Bergeret, A. F. Volkov, and K. B. Efetov, *Phys. Rev. B* **68**, 064513 (2003).
²⁵ V. L. Berezinskii, *JETP Lett.* **20**, 287 (1974).
²⁶ K. D. Usadel, *Phys. Rev. Lett.* **25**, 507 (1970).
²⁷ Y. V. Fominov, N. M. Chtchelkatchev, and A. A. Golubov, *JETP Lett.* **74**, 96 (2001).
²⁸ Y. V. Fominov, N. M. Chtchelkatchev, and A. A. Golubov, *Phys. Rev. B* **66**, 014507 (2002).
²⁹ A. V. Zaitsev, *Sov. Phys. JETP* **59**, 1015 (1984).
³⁰ M. Y. Kupriyanov and V. F. Lukichev, *Sov. Phys. JETP* **67**, 1163 (1988).